Weak Anisotropic X-Ray Magnetic Linear Dichroism at the Eu $M_{4,5}$ Edges of Ferromagnetic EuO(001): Evidence for $4f$-State Contributions

Gerrit van der Laan,[1,2] Elke Arenholz,[3] Andreas Schmehl,[4] and Darrell G. Schlom[5]

[1]*Magnetic Spectroscopy Group, Daresbury Laboratory, Warrington WA4 4AD, United Kingdom*
[2]*Diamond Light Source, Chilton, Didcot, Oxfordshire OX11 0DE, United Kingdom*
[3]*Advanced Light Source, Lawrence Berkeley National Laboratory, Berkeley, California 94720, USA*
[4]*Institut für Physik, Universität Augsburg, Augsburg, Germany*
[5]*Department of Materials Science & Engineering, Penn State University, University Park, Pennsylvania 16802, USA*

(Received 31 July 2007; published 14 February 2008; corrected 15 February 2008)

We have observed a weak anisotropic x-ray magnetic linear dichroism (AXMLD) at the Eu $M_{4,5}$ edges of ferromagnetic EuO(001), which indicates that the $4f$ states are not rotationally invariant. A quantitative agreement of the AXMLD is obtained with multiplet calculations where the $4f$ state is split by an effective cubic crystalline electrostatic field. The results indicate that the standard model of rare earths, where $4f$ electrons are treated as core states, is not correct and that the $4f$ orbitals contribute weakly to the magnetic anisotropy.

DOI: 10.1103/PhysRevLett.100.067403 PACS numbers: 78.70.Dm, 75.10.Dg, 75.70.Ak, 78.20.Bh

The magnetism in rare-earth systems is governed by the magnetic moments of the localized $4f$ orbitals that interact indirectly through delocalized valence electrons. The correlation between localized and itinerant electrons gives rise to a wide variety of electronic, magnetic, and magneto-optical features, often displaying a striking temperature dependence. The magnetic anisotropy, which is at the origin of many interesting and important technological applications, such as magnetic storage devices and sensors, spin-torque nano-oscillators for high-speed spintronics and spin-optics, is still poorly understood in these systems despite decades of intense studies with optical spectroscopy [1].

In the so-called standard model, where the $4f$ states are treated as core states [2,3], the magnetic anisotropy originates from the electrostatic interaction of the $4f$ charge density with the crystalline electric field (CEF) caused by neighboring charges. An applied magnetic field of sufficient strength rotates the direction of the $4f$ total angular momentum and due to the strong spin-orbit interaction the $4f$ charge density then rotates with it. This reorientation of the $4f$ orbitals in the CEF gives an increase in the electrostatic energy that corresponds to the magnetic anisotropy energy. The question that one might ask here is the following. To what extent are the $4f$ orbitals able to rotate freely in order to follow the magnetization, or could it be that they are held back by the CEF and hybridization which couple them to the lattice?

Actually, the latter situation occurs in the $3d$ transition metal group, where the relative strengths of spin-orbit interaction and crystal field are reversed compared to the $4f$ metal group. The $3d$ orbitals are firmly coupled to the lattice, keeping the charge density fixed. The crystal field causes an energy splitting of the $3d$ states into sublevels with different shapes of the charge density, which pins the orbitals to the lattice. The magnetic anisotropy of the $3d$ states is proportional to the difference in expectation value of the orbital magnetic moments along the different magnetization directions [4,5], cf. Fig. 1. It was recently shown that anisotropic x-ray magnetic linear dichroism (AXMLD) provides a sensitive method to determine the influence of the crystal field in $3d$ transition metal oxides [6–8]. X-ray magnetic linear dichroism (XMLD) spectra are the difference between x-ray absorption (XA) spectra with the magnetization oriented parallel and perpendicular to the linear polarization of the x rays. Upon rotation of the crystal the XMLD shows an anisotropy, i.e., an angular

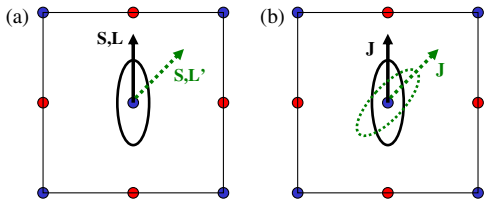

FIG. 1 (color online). Schematics of the magnetic anisotropy for two extreme cases. (a) In $3d$ systems, where the crystalline electrostatic field (CEF) is large and spin-orbit interaction can be treated as a small perturbation, the electron orbitals are firmly coupled to the lattice by CEF and hybridization. The associated orbital moment (L), and through spin-orbit coupling the spin moment (S), are oriented along a well-defined direction, called the easy direction of magnetization. An applied magnetic field rotates S, but the charge density (depicted as the oval shape) remains fixed to the lattice. The difference in expectation value of L along different magnetization directions results in a weak magnetic anisotropy. (b) In $4f$ systems, as described by the standard model, the spin-orbit coupling is strong and the CEF is weak, so that the charge density rotates (oval shape) with the total angular momentum (J) which is aligned along the magnetization direction. The difference in energy associated with different orientations of the charge density results in a large magnetic anisotropy.

dependence with distinctly different spectra at different crystallographic directions.

For the half-filled shell $4f^7$, the spin-orbit interaction and orbital magnetic moment vanish, so that the charge density is no longer coupled to the spin and hence does not rotate with the magnetization direction. This behavior resembles that of the $3d$ series, so that AXMLD might be able to determine the $4f$ crystal field strength and charge anisotropy in this case. Previously, $4f \rightarrow 5d$ optical spectroscopy and magnetization measurements have been used to determine the $4f$ crystal field parameters. However, the large $5d$ crystal field splitting of several eV dwarfs the small $4f$ splitting, which makes the latter difficult to isolate and measure separately by, e.g., using inelastic neutron scattering. Moreover, none of these measurements is element specific. What is really needed to separate the $4f$ from the $5d$ contribution is an electron shell specific probe such as offered by XMLD.

Motivation to study specifically EuO stems from its fascinating properties and technologically importance for spintronics research [9]. It is the only magnetic binary oxide that is thermodynamically stable in contact with silicon and GaN [10]. EuO has a rocksalt structure and is a ferromagnetic semiconductor with a band gap of 1.2 eV and a Curie temperature (T_C) of 69 K [11]. Eu-rich EuO becomes metallic below T_C showing a huge metal-insulator transition (MIT) where the resistivity drops by up to 13 orders of magnitude [12]. An applied magnetic field shifts the MIT temperature, resulting in a colossal magnetoresistance (CMR), which is even larger than in manganite-based oxides. In addition, EuO exhibits one of the highest Faraday rotations. Free carriers can be introduced by photo doping or field doping of the highly spin polarized conduction band [13]. Moreover, EuO with its $[\mathrm{Xe}]4f^7 5d^0 6s^0$ configuration is well suited for our purpose. Its low in-plane magnetic anisotropy allows us to align the magnetization in arbitrary direction using only a moderate external field.

In this Letter, we will determine the energy splitting and asphericity of the $4f$ states in EuO using the AXMLD at the $M_{4,5}$ edges ($3d \rightarrow 4f$ transitions). We show that although the AXMLD is much smaller than for $3d$ transition metal oxides, it can nevertheless be observed and provide novel information. The measurements, which are confirmed by multiplet calculations, show that there is a significant $4f$ anisotropy. This suggests that previously the influence of the valence character of the $4f$ states on the magnetic anisotropy might have been underestimated.

500 nm thick single-crystalline EuO films were grown by thermal evaporation of Eu in presence of 3×10^{-9} Torr O_2 on a 1.3 nm SrO buffer layer deposited on top a clean Si(001) surface [14] and capped *in situ* with 10 nm amorphous Si. The surface near region probed by total electron yield (electron escape depth 5–8 nm [15]) contains 7.5% of Eu_2O_3 that was quantified fitting the experimental data with spectra of the pure compounds [16]. The Eu_2O_3 contribution is due to surface oxidation from the residual oxygen background pressure following the termination of the film growth.

XA spectra were measured in electron yield mode on beam line 4.0.2 at the Advanced Light Source [17] in normal incidence at $T = 15$ K with external fields of 0.5 T by varying the orientation of x-ray linear polarization $\mathbf{E}$ and external magnetic field $\mathbf{H}$ relative to the [100] crystalline axes, cf. inset to Fig. 2(a). The Eu $M_{4,5}$ XA spectrum is shown in Fig. 2(a) and agrees well with previously reported Eu $M_{4,5}$ XA spectra of EuO [16,18], recognizing the small additional intensity around 1133 eV is due to a 7.5% Eu_2O_3.

The XMLD spectrum is defined here as the difference between XA spectra with $\mathbf{H}$ parallel and perpendicular to $\mathbf{E}$, i.e., at angles ϕ and $\phi + 90°$ to the [100] direction,

$$I_{\mathrm{XMLD}}(\phi) = I_{\mathrm{XA}}(\mathbf{H}_\phi, \mathbf{E}_\phi) - I_{\mathrm{XA}}(\mathbf{H}_{\phi+90°}, \mathbf{E}_\phi). \quad (1)$$

For cubic symmetry the angular dependence of the XMLD in the (001) plane is predicted to be [6,7]

$$I_{\mathrm{XMLD}}(\phi) = \tfrac{1}{2}[(I_0 + I_{45}) + (I_0 - I_{45})\cos 4\phi], \quad (2)$$

where $I_0 \equiv I_{\mathrm{XMLD}}(\phi = 0°)$ and $I_{45} \equiv I_{\mathrm{XMLD}}(\phi = 45°)$. The experimental I_0 and I_{45} spectra, which have $\mathbf{E}$ along the [100] and [110] direction, respectively, are shown in Fig. 2(b). According to Eq. (2) all XMLD spectra are a linear combination of these two spectra [7].

The XMLD intensity spans a range of approximately $\pm 15\%$ of the XA near the M_5 edges. This is substantially higher than the XMLD signals observed at the transition metal oxide L_3 edges, which are typically about 5% of the L_3 intensity. On the other hand, only a very weak dependence of the Eu $M_{4,5}$ XMLD signal on the relative orientation of x-ray polarization with respect to the crystal lattice is observed. The most pronounced effect is a small variation in the XMLD spectra near 1156 eV.

To show the angular variation in the XMLD more clearly, we introduce here the residual XMLD spectrum $I^{\mathrm{RES}}_{\mathrm{XMLD}}$ as the measured spectrum with the average XMLD spectrum, $\frac{1}{2}(I_0 + I_{45})$, subtracted,

$$I^{\mathrm{RES}}_{\mathrm{XMLD}}(\phi) \equiv I_{\mathrm{XMLD}}(\phi) - \tfrac{1}{2}(I_0 + I_{45}) = \tfrac{1}{2}(I_0 - I_{45})\cos 4\phi, \quad (3)$$

where the right-hand side is obtained by substituting Eq. (2). Figure 2(c) shows the measured $I^{\mathrm{RES}}_{\mathrm{XMLD}}$ spectra for $0° \leq \phi \leq 45°$, all having the same shape. The modeled angular dependence is displayed by red lines using Eq. (3) with the experimental data for I_0 and I_{45} from Fig. 2(b). Although the angular variation of the XMLD signal is only 1% of the Eu M_5 XA, the experimental data follow very well the expected angular dependence and are as good as in transition metal oxides [7,8].

To confirm the AXMLD at the Eu $M_{4,5}$ edges we compare our experimental data with atomic multiplet calcula-

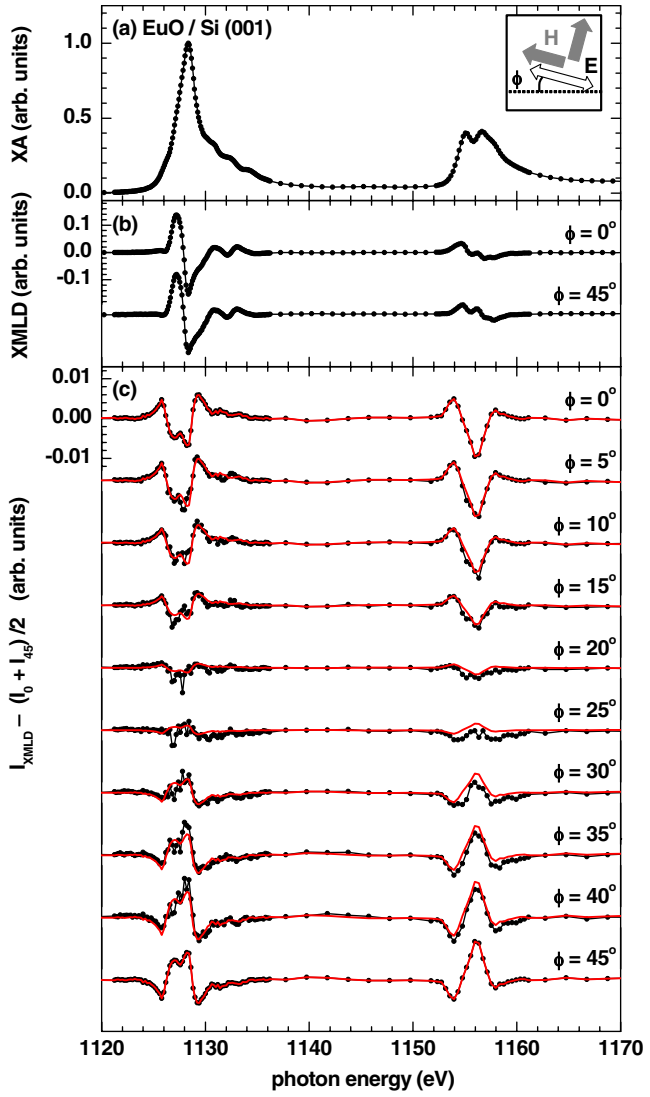

FIG. 2 (color online). Angular dependence of the Eu $M_{4,5}$ XMLD in EuO/Si(001). (a) XA spectrum averaged over all angles ϕ. (b) XMLD spectra I_0 and I_{45} as measured for $\phi = 0°$ and $\phi = 45°$. The experimental geometry is depicted in the inset of (a) indicating the linear polarization **E** (white arrow) at an angle ϕ to the [100] axis (dashed line) and applied external fields **H** (gray arrows) at angles ϕ and $\phi + 90°$, respectively [cf. Eq. (1)]. (c) Residual spectra $I^{\mathrm{RES}}_{\mathrm{XMLD}}$ for $0° \leq \phi \leq 45°$. These are the observed XMLD spectra minus the averaged XMLD according to $I^{\mathrm{RES}}_{\mathrm{XMLD}} = I_{\mathrm{XMLD}}(\phi) - \frac{1}{2}(I_0 + I_{45})$. Symbols indicate the experimental data and (red) lines give the modeled angular dependence using the experimental I_0 and I_{45} spectra.

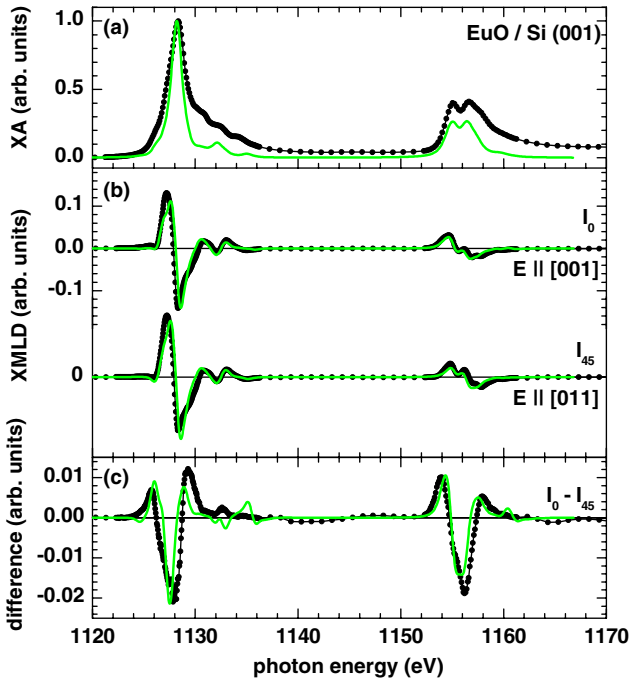

FIG. 3 (color online). Comparison of experimental Eu $M_{4,5}$ XA and XMLD spectra obtained from EuO/Si(001) (black dots) with results of atomic multiplet calculations (green lines) for $V^4_0 = 175$ meV. (a) XA spectrum. (b) Fundamental XMLD spectra I_0 (upper spectrum) and I_{45} (lower spectrum). (c) Difference spectrum $I_0 - I_{45}$.

tions [15,19]. Electric-dipole transitions $3d^{10}4f^7 \rightarrow 3d^9 4f^8$ were calculated in octahedral symmetry with the specified directions of **E** and **H** using the same atomic parameters as before [20]. Figure 3 shows the calculated I_0 and I_{45} and their difference spectrum in comparison with experimental data obtained from EuO(001), using the same scaling for all spectra. The calculations nicely reproduce the experimentally observed features and are in quantitative agreement.

First of all, it is worth to point out that the $3d$ core state, which is initially full, spherical symmetric, and has a binding energy above 1 keV, cannot be responsible for the observed angular dependence. In the case that the CEF is zero, all $4f$ sublevels are degenerate, making the $4f$ state isotropic, so that the $3d \rightarrow 4f$ XMLD is the same at every angle. This is indeed confirmed by the calculations which show that the XMLD is isotropic for the atomic f^7 $^8S_{7/2}$ ground state. Since the spin orbit, Coulomb, and exchange interactions are rotationally invariant, the only source of asphericity is the CEF that splits the $4f$ level into sublevels with different shapes of the charge density. With a half-filled shell as ground state the influence of the CEF on the spectra manifests itself in the final state. Although the strong core-hole interaction, i.e., the $3d$-$4f$ electrostatic interaction, rearranges the spectral distribution, the value of the CEF can be extracted by comparing the experimental results with multiplet calculations, since all interactions are included here on an equal footing [15].

The CEF can be written as a multipole expansion over reduced spherical harmonics, where in cubic symmetry the nonvanishing terms give quadrupolar and octupolar contributions quantified by the parameters V^4_0 and V^6_0, respectively [21]. The CEF will be smaller than the $4f$ spin-orbit

splitting of 0.65 eV and the $4f$ Coulomb interactions [20]. The calculations show that such moderate values of the CEF do not noticeably change the shape and magnitude of the XA, XMCD, and XMLD spectra but only affect the magnitude of the AXMLD, i.e., $I_0 - I_{45}$. In the specific case of the $4f^7 \rightarrow 3d^9 4f^8$ transition, also the shape of the AXMLD hardly changes, and its magnitude is linearly proportional to the value of V_0^4, whereas V_0^6 has a much less influence. This linear dependence allows us to uniquely determine the value of the leading crystal field parameter, and a quantitative agreement with the experimental spectra for EuO is obtained for $V_0^4 = 175$ meV [21]. The calculations furthermore show that $I_0 - I_{45}$ does neither depend on the magnitude of the applied exchange field nor on the size of the $4f$ spin-orbit interaction, while scaling the Slater integrals only gives a modest change in the shape and size of $I_0 - I_{45}$. The symmetry, on the other hand, is of major importance and going from octahedral to tetrahedral environment the $I_0 - I_{45}$ spectrum changes sign while roughly maintaining the same shape. This confirms, at least for f^7, that V_0^4 is the only parameter that controls the AXMLD.

The CEF value of 175 meV obtained by AXMLD exceeds the values quoted for trivalent lanthanides from optical spectroscopy [2,22], but is still an order of magnitude smaller than the crystal field parameters for the $3d$ transition metal oxides. Different to trivalent rare-earth ions, the $4f$ in Eu^{2+} is not screened by $5d$ electrons, making the ionic atomic radius $\sim$20% larger, thereby increasing its CEF strength. The effective energy splitting in the $4f$ includes, apart from the charge potential, anisotropic effects due to hybridization, wave function overlap, band structure, and final-state $4f$-$5d$ interaction. The experimental evidence for a considerable $4f$ splitting clearly shows that the standard model for rare earths cannot be strictly valid and that one needs to take into account the influence of a nonspherical interaction acting on the $4f$ shell. While it has been previously assumed that the $4f$ states should exhibit at least some valence character, thereby breaking the rotational invariance, using AXMLD we have been able to monitor the angular dependence induced by the $4f$ valence character for the first time directly. Generalizing our results to other rare earths, we can conclude that there should be a significant effective CEF, impeding the $4f$ charge density from following the rotation of the magnetization. This finding should have important consequences for the magnetic anisotropy, dynamical processes of spin rotation, and orbital ordering phenomena in rare-earth containing compounds.

To summarize, we have shown that the anisotropy in the XMLD at the Eu^{2+} $M_{4,5}$ edges of EuO(001) is very well described with the model developed for cubic transition metal oxides [7,8]. Multiplet calculations show that the magnitude of the anisotropic XMLD for Eu f^7 is linearly proportional to the effective CEF parameter V_0^4. The experimental spectra evidence a considerable energy splitting of the $4f$ orbitals. The charge anisotropy present in each of the nondegenerate $4f$ states means that pinning of the f states by the local environment becomes feasible and can be tuned by external conditions, chemical doping, and strain for use in device applications.

The Advanced Light Source is supported by the Director, Office of Science, Office of Basic Energy Sciences, of the US Department of Energy under Contract No. DE-AC02-05CH11231.

[1] L. Smentek and B. G. Wybourne, *Optical Spectroscopy of Lanthanides: Magnetic and Hyperfine Interactions* (CRC Press, Boca Raton, 2007).
[2] R. E. Watson and A. J. Freeman, Phys. Rev. **133**, A1571 (1964).
[3] M. S. S. Brookes and B. Johansson, in *Handbook of Magnetic Materials*, edited by K. H. J. Buschow (Elsevier Science, New York, 1993), Vol. 7, p. 139.
[4] P. Bruno, Phys. Rev. B **39**, 865 (1989).
[5] G. van der Laan, J. Phys. Condens. Matter **10**, 3239 (1998).
[6] A. A. Freeman *et al.*, Phys. Rev. B **73**, 233303 (2006).
[7] E. Arenholz *et al.*, Phys. Rev. B **74**, 094407 (2006).
[8] E. Arenholz *et al.*, Phys. Rev. Lett. **98**, 197201 (2007).
[9] A. Mauger and C. Godart, Phys. Rep. **141**, 51 (1986).
[10] A. Schmehl *et al.*, Nat. Mater. **6**, 882 (2007).
[11] B. T. Matthias *et al.*, Phys. Rev. Lett. **7**, 160 (1961).
[12] G. Petrich, S. von Molnr, and T. Penney, Phys. Rev. Lett. **26**, 885 (1971).
[13] E. L. Nagaev, Phys. Status Solidi B **145**, 11 (1988).
[14] J. Lettieri *et al.*, Appl. Phys. Lett. **83**, 975 (2003).
[15] B. T. Thole *et al.*, Phys. Rev. B **32**, 5107 (1985).
[16] E. Negusse *et al.*, J. Appl. Phys. **99**, 08E507 (2006).
[17] A. T. Young *et al.*, J. Synchrotron Radiat. **9**, 270 (2002).
[18] H. Ott *et al.*, Phys. Rev. B **73**, 094407 (2006).
[19] J. B. Goedkoop *et al.*, Phys. Rev. B **37**, 2086 (1988).
[20] The Slater parameters for Coulomb and exchange integrals (reduced to 80% of Hartree-Fock values) and spin-orbit interaction used in the calculation for Eu $4f^7$ are $F^2_{ff} = 10.40$, $F^4_{ff} = 6.49$, $F^6_{ff} = 4.66$, $\zeta_f = 0.161$ and for Eu $3d^9 4f^8$ are $F^2_{ff} = 11.03$, $F^4_{ff} = 6.90$, $F^6_{ff} = 4.95$, $F^2_{df} = 7.00$, $F^4_{df} = 3.23$, $G^1_{df} = 4.92$, $G^3_{df} = 2.88$, $G^5_{df} = 1.99$, $\zeta_f = 0.187$, $\zeta_d = 11.239$ (scaled to 98.53%), all values in eV (from Ref. [15]). The intrinsic lifetime broadening is taken as a Lorentzian with $\Gamma = 0.25(0.5)$ eV for the M_5 (M_4) edge and the instrumental broadening included as a Gaussian with $\sigma = 0.25$ eV.
[21] We define the CEF so that $V_0^4 = 1$ eV splits a one-electron f state in octahedral symmetry into levels A_2 $[f_{xyz}]$, T_2 $[f_{x(z^2-y^2)}, f_{y(x^2-z^2)}, f_{z(x^2-y^2)}]$, and T_1 $[f_{x(5x^2-3r^2)}, f_{y(5y^2-3r^2)}, f_{z(5z^2-3r^2)}]$ with energies $-2/3$, $-1/9$, and $1/3$ eV, respectively.
[22] J. B. Gruber, B. Zandi, and L. Merkle, J. Appl. Phys. **83**, 1009 (1998).